

Nanoporous Carbons from Cypress

- Control of pore structure and application to electric double layer capacitor -

檜から作ったナノポーラスカーボン

-細孔構造の制御と電気二重層キャパシタへの応用-

Eiki Ito^{1,2}, Masahiro Toyoda³ and Michio Inagaki¹
伊藤栄記^{1,2}, 豊田昌宏³, 稲垣道夫¹

Abstract Nanoporous carbons were successfully prepared from cypress chips under a flow of super-heated steam. The cypress charcoals thus obtained were used as electrodes of electric double layer capacitor with 1 M H₂SO₄ electrolyte. Pore structure in cypress charcoals could be controlled by changing carbonization conditions (temperature of super-heated steam, supplying and transferring rates of chips). Under the condition with 15 kg/h supply of chips and 4.7 rpm rotation of transferring paddles, mesopore-rich charcoals with external surface area of about 500 m²/g, which was comparable with microporous surface area, were obtained at 800~870 °C and micropore-rich charcoals with microporous surface area of about 900 m²/g were obtained above 900 °C. Electric double layer capacitor constructed from these cypress charcoals had relatively high capacitance, about 190 F/g with the current density of 50 mA/g and about 140 F/g with 1000 mA/g, which were comparable with the reference activated carbon. The performance rating defined by C₁₀₀₀/C₅₀ was in a range of 0.65~0.85, which was higher than the reference activated carbon.

Keywords : Cypress charcoal; microporous; mesoporous; electric double layer capacitors

1 Introduction

The conservation of forest resources was pointed out to be important for the remediation of environment of the globe. For the conservation, thinning of the forest has to be done periodically. However, this thinning is usually laboring, particularly in steep slope, which is suitable for planting trees, such as cypress and Japanese cedar [1]. In promoting thinning works, effective usage of thinned woods has to be established.

Production of charcoals from various woods has been carried out since prehistoric era and charcoals produced have been used in various applications, such as heating source, adsorbent, medicine, etc. A representative example is activated carbon produced from coconut shells, which has been widely used as adsorbents [2]. Recently, special attentions have been paid on carbon materials contributing to our ecological circumstances and their preparation through the processes gentle for our earth, by calling "eco-carbons" [3]. The production of activated carbons has been carried out from various biomass resources; not only thinned woods but also sawdust, waste woods and bamboos [3-7], which is thought to be one of eco-carbon activity.

Recently new applications of activated carbons in the fields of energy storage and environment protection have been developed [8], which give more severe requirement for pore structure in activated carbons. On the other hand, the applications of the pores larger

than micropores are also developed, such as sorption and recovery of heavy oils [9] and giant biomedical molecules [10]. In order to meet these requirements on pore structure, new processes to produce porous carbons with well-defined pore structure have been proposed; template method [11, 12], defluorination of polytetrafluoroethylene [13, 14], and carbon aerogels [15-17]. In order to produce activated carbons from thinned cypress, we developed a carbonization furnace using super-heated steam [18], which was carried out under the Regional New Consortium R & D Project entitled by "Research and development of the manufacturing system of high performance porous carbons for capacitor from cypress thinning materials of Mikawa district". In the furnace heated by using super-heated steam, carbonization and activation were possible to be carried out at the same time and pore structure of the resultant cypress charcoals was discussed in the relation to the preparation conditions [19, 20],

Activated carbons played an important role to develop one of devices for electric energy storage, *i.e.*, electric double layer capacitors (EDLCs) [21]. In order to enhance the capacitor performance, pore structure in electrode carbons was pointed out to be properly controlled [21-23]. A novel process for the preparation of mesoporous carbons using nano-sized MgO particles was recently established [24-27], of which application to EDLC showed the importance of the presence of mesopores in electrode carbon [28-32].

¹ Faculty of Engineering, Aichi Institute of Technology, Yakusa, Toyota 470-0392, Japan

² Intellectual Property Bank Corp., Toranomon, Minato-ku, Tokyo 105-0001, Japan

³ Faculty of Engineering, Oita University, Dannoharu 700, Oita 870-1192, Japan

Activated charcoals were tried to be applied to EDLCs [33]. EDLC performance using the cypress charcoals prepared under super-heated steam were also studied [34, 35].

In the present paper, the results on cypress charcoals, which are obtained under our research project mentioned above, are summarized by focusing on how pore structure can be controlled and what performance can be obtained as the electrode in EDLC.

2 Experimental

2.1 Preparation of cypress charcoals

For the carbonization of cypress chips under super-heated steam a pilot-plant scale apparatus was constructed, as schematically shown in Fig. 1.

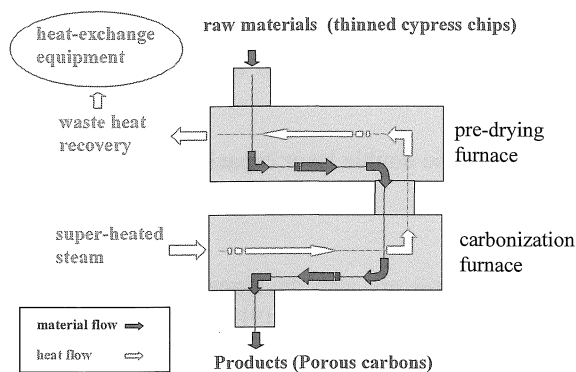


Fig. 1 Construction of the apparatus for the carbonization under super-heated steam.

This apparatus consists of the generator of super-heated steam, the carbonization furnace using high-temperature steam, the pre-drying furnace for cypress chips using low-temperature steam, and the pyrolytic incinerator for wasted gases. The size of the carbonization furnace is 267 mm in diameter and 2.2 m in length. Cypress chips and their carbonized ones are transferred from pre-drying part to carbonization part and finally to the outlet of the furnace by rotating paddles with a constant rate, where super-heated steam is flowing in contrary direction. The details on the performance of the carbonization apparatus and also on the carbonization procedure under a flow of super-heated steam were reported in our previous paper [18].

The original cypress chips had a size of about 10~20 mm x 10~60 mm x 2~10 mm. Temperature for the carbonization was determined at the inlet of super-heated steam to the carbonization furnace and super-heated steam was supplied with a constant rate of 125 kg/h. Carbonization temperature employed in the present work was in the range of 700~950 °C. The cypress chips of 30 or 15 kg were supplied during 1 hour and transferred to carbonization furnace through

pre-drying furnace by the rotation of paddles with a rate of either 4.7, 9.4 or 18.8 rpm.

After carbonization, the charcoals obtained was pulverized in a ball mill to the particle size less than 75 μm and subjected to different examinations.

2.2 Characterization of pore structure

Pore structure of the charcoal was evaluated through the analysis of adsorption/desorption isotherm of N_2 gas at 77 K by using BET, α_s , BJH and DFT methods. By BET analysis on the data measured at the relative pressure P/P_0 of N_2 gas below 0.2, surface area S_{BET} was determined. From α_s plot referring to a standard carbon black, total surface area S_{total} , external surface area $S_{\text{ext.}}$ and micropore volume $V_{\text{micro.}}$ were determined, as shown in Fig. 2. From the balance between S_{total} and $S_{\text{ext.}}$, microporous surface area $S_{\text{micro.}}$ was calculated. External surface area $S_{\text{ext.}}$ was the surface area due to the pores larger than 2 nm, but its main part is caused by the surface area due to mesopores (2~50 nm size).

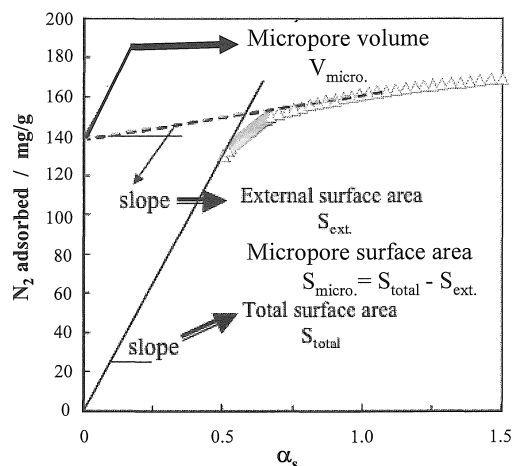


Fig. 2 An example of α_s plot on a cypress charcoal

The charcoals prepared were also analyzed by BJH method using desorption branch of the isotherm of N_2 gas, in order to evaluate surface area and volume of mesopores. From the cumulative curves, surface area and pore volume due to mesopores $S_{\text{meso.}}$ and $V_{\text{meso.}}$ were determined by separating from those due to micropores (the pore size less than 2 nm) $S_{\text{micro.}}$ and $V_{\text{micro.}}$. From BJH and DFT analysis, pore size distribution in mesopore region and that in micropore region, respectively, were determined.

2.3 Performance in electric double layer capacitor

For the determination of the performance of electric double layer capacitor (EDLC) for the cypress charcoals, the electrode was prepared by mixing the charcoal with acetylene black as an electrical conductor and poly(tetrafluoroethylene) (PTFE) as a binder in a mass ratio of 80:10:10, which were blended to be

homogeneous by using N-methyl-2-pyrrolidone as a solvent. The mixture was pressed and rolled to get the film in approximate thickness of 100 μm and then dried at 100 $^{\circ}\text{C}$ for 1 h under vacuum. Three-electrode test cell was used with the film of cypress charcoal thus prepared as a working electrode, 1 mol/L H_2SO_4 as electrolyte, Ag/AgCl as a reference electrode and a platinum plate as a counter electrode. For these sample electrodes the potential-time curves (hereafter, called charge-discharge cycles) in the potential window from 0.0 to 1.0 V were carried out at room temperature. The capacitance of the sample electrode was calculated from charge-discharge curves at 0.2 to 0.8 V. The current density employed for the measurement of capacitance was 50~1000 mA/g. Charge-discharge cycles were performed as follows; 5 cycles with a current density of 50 mA/g, 100 cycles with 100, 200 and 500 mA/g and then 1000 cycles with 1000 mA/g. The preparation process of carbon electrode sheet and the construction of the electrochemical test cell used are schematically shown in Fig. 3. Rate performance of the sample electrode was expressed as the ratio of the capacitance measured with a current density of 1000 mA/g, C_{1000} , to that with 50 mA/g, C_{50} (performance rating C_{1000}/C_{50}).

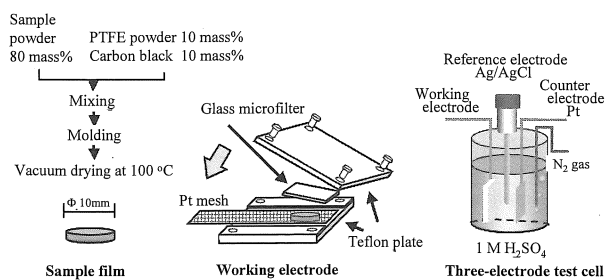


Fig. 3 Preparation procedure for electrode sheet, construction of an electrode and an electrochemical test cell for the measurement of behavior in electric double layer capacitor

In the present work, an activated carbon, which was commercially available as electrode material for EDLC, was used for comparison.

3 Results

3.1 Pore structure of cypress charcoals

In Fig. 4, adsorption/desorption isotherms are shown on the cypress charcoals prepared at different temperatures under super-heated steam.

The charcoals obtained at 700~950 $^{\circ}\text{C}$ show an abrupt increase in adsorbed amount at low relative pressure P/P_0 , more pronounced above 780 $^{\circ}\text{C}$, suggesting that these charcoals contain certain amount of micropores. Above 780 $^{\circ}\text{C}$ the isotherm changes from Type I to Type IV gradually, showing a slight

hysteresis between adsorption and desorption branches. These isotherms suggest the formation of the pores larger than micropores, mainly mesopores, in the charcoals. The isotherm for the charcoal obtained at 946 $^{\circ}\text{C}$ suggests the presence of a large amount of micropores, comparable with the charcoal at 843 $^{\circ}\text{C}$, but a small amount of mesopores, much less than that at 843 $^{\circ}\text{C}$.

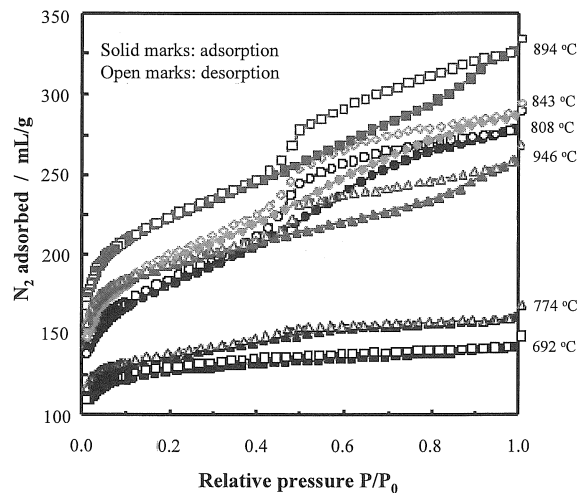


Fig. 4 Adsorption/desorption isotherm of N_2 at 77 K.

For cypress charcoals prepared at different temperatures under three different conditions (different supplying and transferring rates, R_s and R_t), surface areas determined by BET and α_s plot analyses are listed in Table 1, together with the reference activated carbon.

In Figs. 5a to 5c, S_{total} , S_{micro} , and S_{ext} are plotted against carbonization temperature under different conditions for supplying and transferring rates of cypress chips.

High values of S_{BET} and S_{total} of about 1000 m^2/g could be obtained. Total surface area S_{total} consists of mainly the surface area due to micropores S_{micro} . However, it has to be pointed out that some of cypress charcoals have relatively high external surface area S_{ext} , for which mesopores are responsible.

Carbonization of the same cypress chips in Ar gas flow did not give high S_{total} , less than 500 m^2/g [19]. However, S_{total} of more than 1000 m^2/g was obtained above 800 $^{\circ}\text{C}$ by the carbonization under super-heated steam, as shown in Fig. 5. The changes in BET surface area S_{BET} with carbonization temperature under different carbonization conditions were very similar to those in S_{total} shown in Fig. 5, although the absolute values of both surface areas were not the same [18, 19]. This result reveals that activation is performed under the flow of super-heated steam above the temperature of 800 $^{\circ}\text{C}$, being associated with carbonization.

Table 1 Preparation condition, surface area and EDLC performance of cypress charcoals.

T (°C)	Rs (kg/h)	Rt (rpm)	S _{BET} (m ² /g)	Surface area by α_s plot (m ² /g)			EDLC capacitance (F/g)					C ₁₀₀₀ /C ₅₀
				S _{total}	S _{ext.}	S _{micro.}	50*	100*	200*	500*	1000*	
780	15	4.7	462	502	62	440	--	--	--	--	--	--
788			515	563	114	449	--	--	--	--	--	--
800			776	840	410	430	--	--	--	--	--	--
828			827	919	422	497	--	--	--	--	--	--
832			842	941	433	509	--	--	--	--	--	--
832			846	912	502	410	180	171	163	152	143	0.79
849			874	968	471	498	187	175	165	153	143	0.76
849			836	919	445	475	--	--	--	--	--	--
874			985	1057	489	569	187	166	152	137	133	0.73
922			956	1078	204	874	--	--	--	--	--	--
925			935	1041	177	864	--	--	--	--	--	--
939			1035	1180	335	846	189	163	148	136	130	0.69
692			30	9.4	481	561	57	504	--	--	--	--
746	440	533			71	462	--	--	--	--	--	--
755	468	577			103	475	--	--	--	--	--	--
774	512	597			101	496	--	--	--	--	--	--
808	661	733			259	474	165	150	142	128	114	0.69
809	649	748			266	483	164	152	140	126	110	0.67
843	709	817			261	557	167	151	138	125	114	0.68
844	835	992			272	720	204	183	170	156	143	0.70
849	714	845			265	580	180	154	138	126	113	0.63
887	836	983			287	696	--	--	--	--	--	--
894	781	928			247	681	171	163	155	143	130	0.76
902	804	959			243	716	186	171	156	142	129	0.69
937	762	918			217	701	193	180	170	153	138	0.72
946	695	857	153	705	165	153	143	132	132	0.80		
748	30	18.8	553	631	155	476	86	85	80	57	58	0.67
809			531	602	175	427	92	89	88	77	67	0.73
837			555	607	221	386	110	105	101	90	78	0.71
864			924	1043	271	773	191	169	162	147	134	0.70
Activated carbon			1587	1717	208	1508	229	206	185	159	137	0.60

T: carbonization temperature (Temperature of super-heated steam supplied), Rs: supplying rate of chips, Rt: transferring rate of chips, C₁₀₀₀/C₅₀: performance rating and * current density during charge-discharge cycle (mA/g)

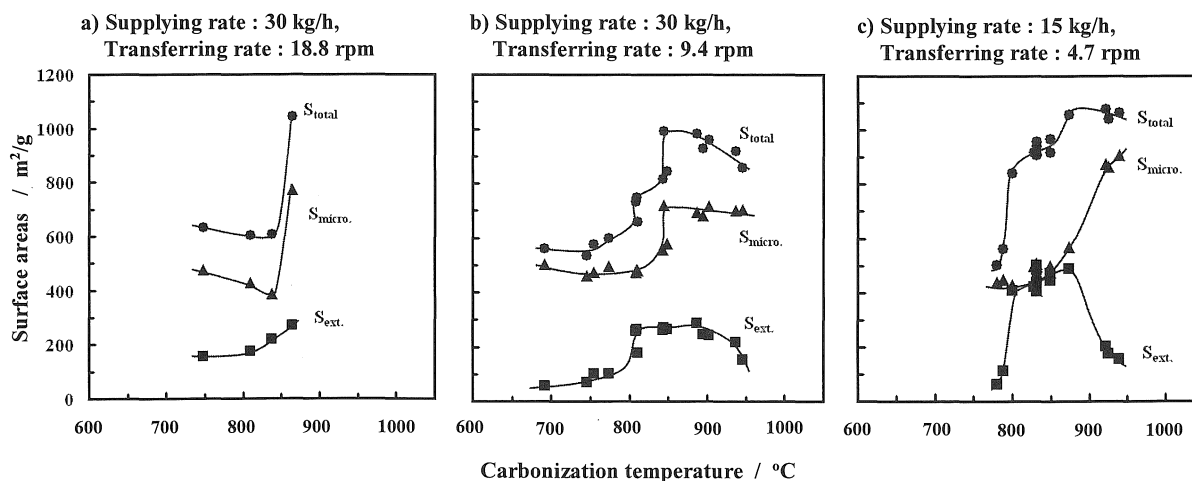


Fig. 5 Changes in total surface area S_{total} , microporous surface area S_{micro} , and external surface area $S_{ext.}$ in cypress charcoals with carbonization temperature under different supplying and transferring conditions.

Under the condition with supplying rate of 30 kg/h and transferring rate of 9.4 rpm, carbonization of cypress chips were carried out in three independent

series. The reproducibility in pore parameters S_{total} , S_{micro} , and $S_{ext.}$ are excellent [19]. In Fig. 5b, the experimental points obtained in these three series of ex-

periments are plotted by the same marks.

As shown in Figs. 5a to 5c, the changes in S_{total} , $S_{micro.}$ and $S_{ext.}$ with carbonization temperature depend strongly on carbonization condition (supplying and transferring rates) of cypress chips. Three conditions were selected, supplying the 30 kg chips during 1 h with rotation rate of 18.8 and 9.4 rpm (Figs. 5a and 5b, respectively) and supplying a smaller amount of chips during 1 h (15 kg/h) with a slower rotation of 4.7 rpm (Fig. 5c). Actually, the charcoal production under the condition with 30 kg/h and 4.7 rpm was carried out, but the quality of obtained charcoals, measured by yield and pore structure, was not stable, probably because chips and/or charcoals in the pre-drying and carbonization furnaces could not transfer in a steady rate mainly due to unbalance between supplying speed and transferring speed of chips. The condition shown in Fig. 5a (30 kg/h and 18.8 rpm) may be called fast carbonization, the condition in Fig. 5b (30 kg/h and 9.4 rpm) is medium carbonization and the condition in Fig. 5c (15 kg/h and 4.7 rpm) is mild carbonization.

Under fast carbonization condition (Fig. 5a), a rapid increase in $S_{micro.}$, consequently in S_{total} , is observed above 850 °C. Under medium condition (Fig. 5b), however, a rapid increase in S_{total} occurs in two steps, at around 800 and 850 °C, the former corresponding to the increase in $S_{ext.}$ and the latter to that in $S_{micro.}$. Under mild condition (Fig. 5c), $S_{ext.}$ increases abruptly up to 500 m²/g at around 800 °C and so S_{total} also increases, though $S_{micro.}$ does not show appreciable increase. Above 900 °C, $S_{micro.}$ shows a rapid increase, but $S_{ext.}$ decreases and as a consequence S_{total} increases a little.

These results suggest that either mesoporous or microporous carbon can be prepared by changing carbonization condition (temperature of super-heated steam, supplying and transferring rates of chips); mesopore-rich charcoals at around 800 °C and micropore-rich charcoals above 850 °C under either medium or mild condition. Under fast condition, abrupt increase in $S_{ext.}$ was difficult to be observed and a high $S_{micro.}$ was observed above 850 °C.

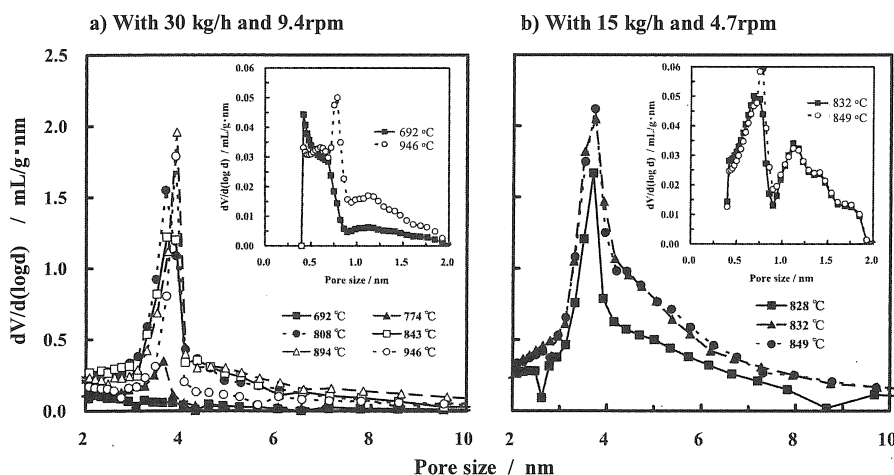


Fig. 6 Pore size distribution of cypress charcoals prepared under super-heated steam.

In Figs. 6a and 6b, pore size distribution in mesopore region is shown for cypress charcoals prepared under medium and mild conditions, respectively, together with that in micropore region as inserted figures. Cypress charcoals prepared under super-heated steam have relatively sharp distribution at around 4 nm, a little broader in the charcoals prepared under mild condition than those under medium condition. In micropore region, a sharp distribution is observed at around 0.8 nm in all charcoals prepared at a temperature above 800 °C.

3.2 Performance in electric double layer capacitor

In Fig. 7, charge-discharge curves (in exact meaning, potential-time curves) with a current density of 50 and 1000 mA/g are shown for the cypress charcoal prepared at 939 °C. No IR drop is detected and pretty good linearity is observed.

In Table 1, EDLC capacitance measured with different current densities are listed, together with performance rating C_{1000}/C_{50} . Some of cypress charcoals could give relatively high EDLC capacitance, about 200 F/g with a current density of 50 mA/g, and performance rating C_{1000}/C_{50} is also relatively high as 0.7.

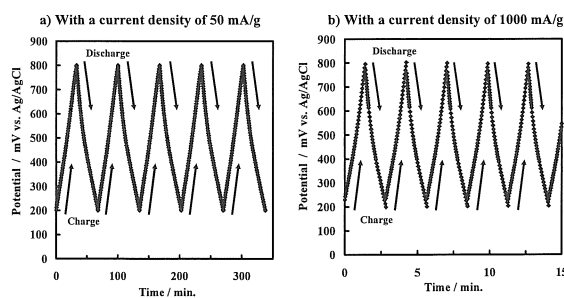


Fig. 7 Potential-time curves (charge-discharge curves).

In Fig. 8, the dependence of capacitance on current density is shown for some cypress charcoals, including the reference activated carbon. Pore parameters, $S_{\text{ext.}}$ and $S_{\text{micro.}}$, of the samples are listed in the figure.

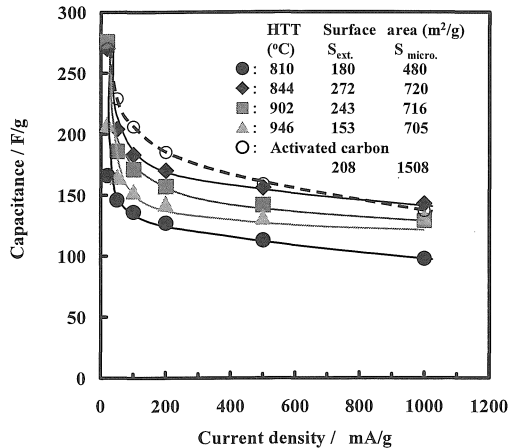


Fig. 8 Dependences of capacitance on current density for cypress charcoals and activated carbon.

With low current density as 50 mA/g, *i.e.*, slow charge-discharge, cypress charcoals prepared above 800 °C give a little smaller EDLC capacitance with the reference activated carbon, even though the difference in surface areas between cypress charcoals and the reference activated carbon is very large. With high current density as 1000 mA/g, *i.e.*, rapid charge-discharge, however, the cypress carbons show relatively high capacitance, comparable to the activated carbon.

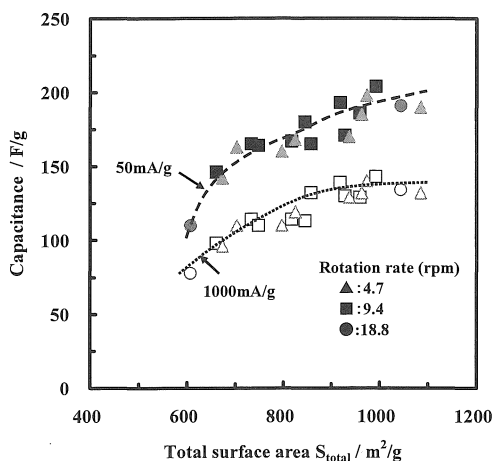


Fig. 9 Dependences of capacitance with a current density of 50 and 1000 mA/g on total surface area for cypress charcoals.

On cypress charcoals prepared, it is seen that capacitance decreases very rapidly with increasing current density up to about 200 mA/g, but gradually above

200 mA/g, although the reference activated carbon shows marked decrease in capacitance even above 200 mA/g.

In Fig. 9, capacitance measured with a current density of 50 and 1000 mA/g is plotted against S_{total} of the electrode carbon. With increasing S_{total} , capacitance increases gradually and tends to saturate above 900 m²/g. On these relations, no difference due to different carbonization conditions is observed, suggesting that capacitance of EDLCs is governed mainly by the surface area of electrode carbon.

4 Discussion

4.1 Pore structure in cypress charcoals prepared

From the view point related with pore structure control and EDLC performance, medium and mild carbonization conditions are more interesting. For the production of porous carbons with a high surface area, the fast carbonization condition (Fig. 5a) might not be advantageous because relatively high temperature as 900 °C is required in order to get high microporous surface area.

Under medium condition (Fig. 5b), S_{total} increases in two steps at 800 and 850 °C, which are corresponding to the abrupt increase in $S_{\text{ext.}}$ and $S_{\text{micro.}}$, respectively. At 800 °C, $S_{\text{ext.}}$ can reach close to 300 m²/g, but $S_{\text{micro.}}$ is less than 500 m²/g and consequently S_{total} is a little more than 700 m²/g. Above 850 °C, $S_{\text{ext.}}$ levels off at about 250 m²/g, but $S_{\text{micro.}}$ increases up to 700 m²/g, and so S_{total} reaches 1000 m²/g. However, further carbonization makes surface areas smaller, particularly $S_{\text{ext.}}$ decreasing markedly. Under fast carbonization condition (Fig. 5a), the values of S_{total} , $S_{\text{micro.}}$ and $S_{\text{ext.}}$ corresponding to those obtained under medium condition can be obtained, but a high temperature above 850 °C is required.

Under mild carbonization condition (Fig. 5c), S_{total} increases at about 800 °C and then saturated at about 1050 m²/g above 850 °C. $S_{\text{ext.}}$ increases abruptly to more than 400 m²/g at 800 °C, but decreases above 900 °C down to about 150 m²/g. In contrast, $S_{\text{micro.}}$ does not increase up to 850 °C, but then increases up to 900 m²/g. This figure demonstrates clearly that the increase in S_{total} at about 800 °C is due to the increase in $S_{\text{ext.}}$. $S_{\text{ext.}}$ reaches more than 400 m²/g at the temperature of 800 ~ 870 °C, although only 20 ~ 60 m²/g in Ar gas flow [19]. It is interesting to be pointed out that $S_{\text{ext.}}$ is comparable with $S_{\text{micro.}}$ in this temperature range. Above 870 °C, S_{total} is kept almost constant because of the compensation of the decrease in $S_{\text{ext.}}$ by the increase in $S_{\text{micro.}}$. BJH analysis on these cypress charcoals gave exactly the same results, large values of mesoporous surface area $S_{\text{meso.}}$ and mesopore volume $V_{\text{meso.}}$ at the temperature range of 800~870 °C, suggesting that main part giving the value of $S_{\text{ext.}}$ is due to mesopores.

On Fig. 5, it has to be pointed out the fact that

the increase in $S_{ext.}$, in other words, the development of mesopores, occurs in advance of the increase in $S_{micro.}$ in cypress charcoal, $S_{ext.}$ increasing at around 800 °C and $S_{micro.}$ above 850 °C (Figs. 5b and 5c). In conventional activation process of various carbon materials using either gases or chemicals, mesopores can be created through enlarging micropores, in other words, mesopores are able to be formed as a sacrifice for micropores. In the carbonization of cypress under super-heated steam, however, micropores are formed after the formation of mesopores, phenomenologically micropores being formed as a sacrifice for mesopores.

Fig. 5 reveals also that pore structure in cypress charcoal can be controlled by changing the carbonization condition (temperature of super-heated steam for carbonization, and supplying and transferring rates of cypress chips); under mild condition (supplying rate of 15 kg/h and transferring rate of 4.7 rpm) mesopore-rich charcoals with relatively high external surface area are obtained at a temperature range of 800 ~ 870 °C, but micropore-rich charcoals above 900 °C.

In Figs. 6a) and 6b), pore size distributions in mesopore and micropore regions, were shown for the cypress charcoals prepared under super-heated steam at different conditions. Under medium carbonization condition, the charcoals prepared above 800 °C are mesoporous, showing a high population at 4 nm size. Above 900 °C, the population at 4 nm decreases a little and micropores with the size of about 0.8 nm appear, these pores contributing the increase in $S_{micro.}$ On cypress charcoals prepared in Ar gas flow, a similar pore size distribution in mesopore region was observed, but the population of these pores was very low, almost one order of magnitude smaller than that under super-heated steam.

4.2 Performance in electric double layer capacitor

To understand the dependence of EDLC capacitance on pore structure, the following relation was proposed [36], where the capacitance observed, $C_{obs.}$, was divided into the contributions from microporous

surface, $C_{micro.}$, and external surface, $C_{ext.}$.

$$C_{obs.} = C_{micro.} \cdot S_{micro.} + C_{ext.} \cdot S_{ext.}$$

In Fig. 10, the relations between $C_{obs.}/S_{ext.}$ and $S_{micro.}/S_{ext.}$ for current density of 50 and 1000 mA/g are shown on the cypress charcoals.

For every current density employed in the present work, a good linear relation between $C_{obs.}/S_{ext.}$ and $S_{micro.}/S_{ext.}$ was obtained, as shown for 50 and 1000 mA/g in Fig. 10. From the slope and the intercept of this relation, the capacitance contribution from microporous surface, $C_{micro.}$, and that from external surface, $C_{ext.}$, can be obtained, respectively; 0.17 and 0.28 F/m² for the current density of 50 mA/g and 0.13 and 0.18 F/m² for 1000 mA/g, respectively. Both $C_{micro.}$ and $C_{ext.}$ depends on current density and are in the same order of magnitude, but the former is a little smaller than the latter.

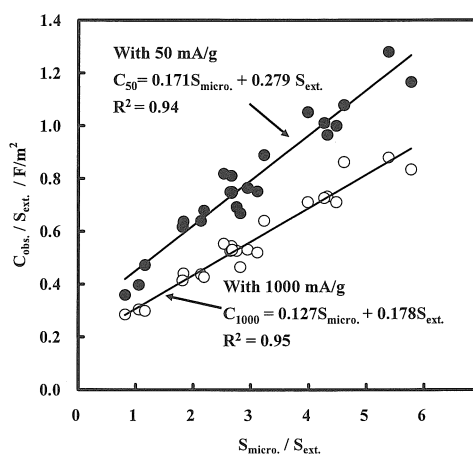


Fig. 10 Relation between $C_{obs.}/S_{ext.}$ and $S_{micro.}/S_{ext.}$ for cypress charcoals prepared under super-heated steam.

In Table 2, the data on $C_{micro.}$ and $C_{ext.}$, which have been published in different literatures, are listed up with electrolyte, sample carbon and method for capacitance determination.

Table 2 Comparison of the contributions (F/m²) of microporous and external surface areas, $C_{micro.}$ and $C_{ext.}$, in aqueous and non-aqueous electrolytes to the capacitance observed $C_{obs.}$.

Electrolyte solution	Sample carbon	Method of capacitor determination and current	$C_{micro.}$	$C_{ext.}$	$C_{ext.}/C_{micro.}$	Reference	
5 M KOH aqueous solution	Microbeads	P-t curve, 5 mA	0.195	0.74	3.8	36	
	Carbon fibers		0.145	0.075	0.5		
6 M KOH aqueous solution	Activated carbons from coals	P-t curve, 160 mA/g	0.101	0.091	0.9	37	
1 M H ₂ SO ₄ aqueous solution			0.098	0.231	2.4		
1 M PC solution of Et ₃ MeNBF ₄	Air-oxidized carbon spheres	P-t curve	20mA	0.017	0.187	11	38
			200 mA	0.008	0.116	15	
1 M H ₂ SO ₄ aqueous solution	Cypress charcoal prepared under super-heated steam	P-t curve	50 mA/g	0.17	0.28	1.6	Present work
			1000 mA/g	0.13	0.18	1.4	

The values of observed capacitance $C_{obs.}$ and consequently capacitance contributions $C_{micro.}$ and $C_{ext.}$, are strongly governed by the electrolyte used, methods of capacitance measurement and also methods of measurement of surface areas corresponding to $S_{micro.}$ and $S_{ext.}$. Therefore, the data summarized in Table 2 have to be discussed by using the ratio between two contributions, $C_{ext.}/C_{micro.}$. In aqueous electrolyte, the ratio $C_{ext.}/C_{micro.}$ is around .1, although large scattering is observed. In non-aqueous electrolyte, on the other hand, the ratio $C_{ext.}/C_{micro.}$ is more than 10. This is very reasonable because cation and anion of most aqueous electrolytes are small, but those of non-aqueous electrolyte are large, the larger ions are the more difficult to be adsorbed into small pores (micropores) with the larger current density.

In Fig. 11, therefore, the capacitance contributions $C_{micro.}$ and $C_{ext.}$ measured on the cypress charcoals are plotted against current density. $C_{ext.}$ is a little larger than $C_{micro.}$ for all current densities examined, which is very reasonable because the adsorption of ions onto external surface, which is due to large-sized pores, is easier than that onto the surface due to micropores. The result that both contributions become smaller with increasing current density from 50 to 1000 mA/g are also able to be explained by the fact that the adsorption of ions onto pore surfaces becomes the more difficult by the faster charge-discharge.

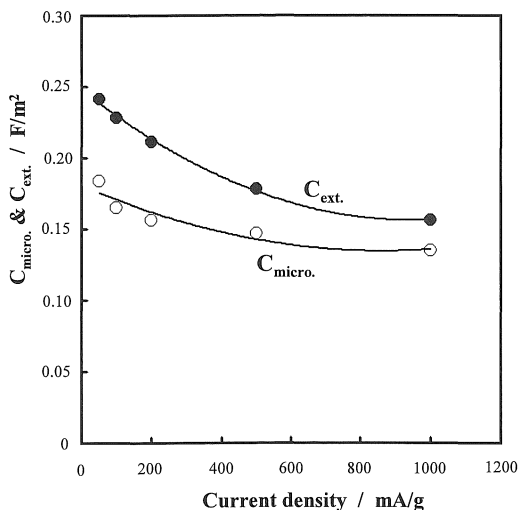


Fig. 11 Changes of the contribution of microporous surface $C_{micro.}$ and that of external surface $C_{ext.}$ with current density for charge-discharge.

It was pointed out in different papers that the presence of mesopores in the electrode carbon was important factor to get high rate performance in EDLC. In Fig. 12, performance rating C_{1000}/C_{50} is plotted against $S_{ext.}/S_{total}$, *i.e.*, relative external surface area.

Most of cypress charcoals prepared in the present work show a value of C_{1000}/C_{50} between 0.65 and 0.85.

but the reference activated carbon gives about 0.60. The charcoal with almost equal values of $S_{micro.}$ and $S_{ext.}$, *i.e.*, $S_{ext.}/S_{total}$ of about 0.5, gives a high performance rating as 0.85. A good rate performance of cypress charcoals is reasonably supposed to be due to high external surface area $S_{ext.}$.

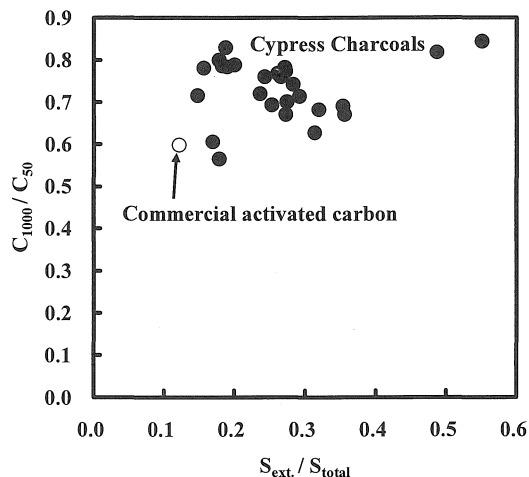


Fig. 12 Relation between performance rating C_{50}/C_{1000} and relative external surface area $S_{ext.}/S_{total}$.

5 Conclusions

Nanoporous carbons were successfully prepared from cypress chips under super-heated steam. Carbonization and activation of cypress proceeded above 800 °C at the same time and high BET surface area as 1000 m²/g was obtained. The pore structure in cypress charcoal was found to be controlled by selecting carbonization condition, *i.e.*, temperature of super-heated steam and supplying and transferring rates of chips. Under a mild condition with supplying cypress chips by 15 kg/h and 4.7 rpm rotation of the transferring paddles, the cypress charcoals prepared at carbonization temperature of 800~870 °C were characterized by a large external surface area, as larger as 400~500 m²/g, which is comparable with microporous surface area.

Cypress charcoals prepared under super-heated steam were used in electric double layer capacitor (EDLC) with 1 M H₂SO₄ electrolyte. Gravimetric EDLC capacitance of cypress charcoals prepared above 800 °C was about 190 F/g with the current density of 50 mA/g, which was a little smaller than that of the reference activated carbon, but about 140 F/g with 1000 mA/g, comparable to the activated carbon. The capacitance observed was explained by almost equivalent contributions from microporous surface $C_{micro.}$ and external surface $C_{ext.}$. Performance rating defined by C_{1000}/C_{50} was in the range of 0.65~0.85, even though the reference activated carbon gave the value of 0.60. The presence of mesopores in electrode carbon was shown to be important for giving a high performance

rating; the cypress charcoal, which have almost equal values of microporous surface area to external surface area, gives a high performance rating C_{1000}/C_{50} of about 0.85.

Acknowledgement

The present work was performed as a part of Regional New Consortium R & D Project "Research and development of the manufacturing system of high performance porous carbons for capacitor from cypress thinning materials of Mikawa district", which was supported by The Chubu Bureau of The Ministry of Economy, Trade and Industry of Japan for FY 2005~2006. The present authors would like to express sincere thanks to The Ministry for financial support and also to the members of the R & D project for their cooperation and encouragement.

References

- [1] Home page of Forestry Agency, The Ministry of Agriculture, Forestry and Fisheries of Japan, <http://www.rinya.maff.go.jp/index.html> (March 12th, 2007)
- [2] Sanada Y, Suzuki M, Fujimoto K. *Activated carbons: Fundamentals and Applications*, Koudansha, 1992 [in Japanese].
- [3] Abe I. *TANSO* 2005 [No. 220] 310-318.
- [4] Abe I. *TANSO* 2004 [No. 211] 21-29.
- [5] Sugamoto K, Matsushita Y, Fujimoto S and Matsui T. *TANSO* 2004 [No. 212]: 69-74.
- [6] Inagaki M, Nishikawa T, Sakuratani K, Katakura T, Konno H and Morozumi E. *Carbon* 42 (2004) 890-893.
- [7] Abe I, Hasegawa T, Shibutani Y and Iwasaki S. *TANSO* 2004 [No. 215] 241-245.
- [8] Conway B E, *Electrochemical supercapacitors*, Kluwer Academic/Plenum Publishers (1999).
- [9] Toyoda M, Iwashita N and Inagaki M, *Chemistry and Physics of Carbon*, L. R. Radovic, Ed. (in press).
- [10] Kang F, Zheng Y, Zhao H, Wang H, Wang L, Shen W and Inagaki M, *New Carbon Materials*, 18 (2003) 161-173.
- [11] Kyotani T, Porous Carbons. In: *Carbon Alloys*. Yasuda E, Inagaki M, Kaneko K, Endo M, Oya A, Tanabe Y, Eds. Amsterdam; Elsevier (2003) p. 109-27.
- [12] Shi Z-G, Feng Y-Q, Xu L and Da S-L, *Carbon* 41 (2003) 2668-2670.
- [13] Shiraishi S, Kurihara H, Tsubota H, Oya A, Soneda Y and Yamada Y, *Electrochem. Solid-State Lett.* 4 (2001) A5-A8.
- [14] Tanaike O, Hatori H, Yamada Y, Shiraishi S and Oya A, *Carbon* 41 (2003) 1759-1764.
- [15] Hanzawa Y, Kaneko K, Yoshizawa N, Pekala R W and Dresselhaus M S, *Adsorption* 4 (1998) 187-195.
- [16] Tamon H, Ishizaki H, Mikami M and Okazaki M, *Carbon* 35 (1997) 791-796.
- [17] Yamamoto T, Nishimura T, Suzuki T and Tamon H, *Drying Tech.* 19 (2001) 1319-1333.
- [18] Ito E, Sano T, Kouchi I, Okuda M, Nakano T, Umemura M, Niwa Y, Yashio M, Azuma, Y, Yamaji Y, Toyoda M and Inagaki M. *TANSO* 2007 [No. 229] 249-254.
- [19] Ito E, Yokoi T and Inagaki M. *TANSO* 2007 [No. 229] 255-260.
- [20] Ito E, Kouchi I, Mozia S, Okuda M, Nakano T, Toyoda M and Inagaki M, *New Carbon Materials* 22 (2007) 199-205.
- [22] Frackowiak E. and Beguin F. *Carbon* 39 (2001) 937-950.
- [21] Shiraishi S, Kurihara H, Shi L, Nakayama T and Oya A, *J. Electrochem. Soc.* 149 (2002) A855-A861.
- [23] Centeno T A, Sevilla M, Fuertes A B, Stoeckli F, *Carbon* 43 (2005) 3012-3015.
- [24] Morishita T, Suzuki T, Nishikawa T, Tsumura T and Inagaki M, *TANSO* 2005 [No. 219] 226-231.
- [25] Morishita T, Suzuki T, Nishikawa T, Tsumura T and Inagaki M, *TANSO* 2006 [No. 223] 220-226.
- [26] Morishita T, Ishihara K, Kato M and Inagaki M, *TANSO* 2007 [No. 226] 19-24.
- [27] Inagaki M, Kato M, Morishita T, Morita K and Mizuuchi K, *Carbon* 45 (2007) 1121-1124.
- [28] Morishita T, Soneda Y, Tsumura T and Inagaki M, *Carbon* 44 (2006) 2360-2367.
- [29] Morishita T, Ishihara K, Kato M, Tsumura T and Inagaki M, *Carbon* 45 (2007) 209-211.
- [30] Fernandez J A, Morishita T, Toyoda M, Inagaki M, Stoeckli F and Centeno T A, *J. Power Sources* 175 (2008) 675-679.
- [31] Wang, L., Morishita T., M. Toyoda and Inagaki, *Electrochim. Acta* (in press).
- [32] Wang L, Toyoda M and Inagaki M, *Ads. Sci. Tech.* (in press).
- [33] Asakura R, Kondo T, Morita M, Hatori H and Yamada Y, *TANSO* 2004 [No. 215] 231-235.
- [34] Ito E, Nakamura H and Inagaki M. *TANSO* 2008 [No. 231] 8-12.
- [35] Ito E, Mozia S, Toyoda M and Inagaki M. *New Carbon Mater.* 22 (2007) 321-326.
- [36] Shi H, *Electrochim. Acta* 41 (1996) 1633-1639.
- [37] Gryglewicz G, Machnikowski J, Lorenc-Grabowska E, Lota G and Frackowiak E, *Electrochim. Acta* 50 (2005) 1197-1206
- [38] Wang L, Fujita M and Inagaki M, *Electrochim. Acta* 51 (2006) 4096-4102.